

68th Conference of the Italian Thermal Machines Engineering Association, ATI2013

Aerodynamic Characterization of a Wells Turbine Under Bi-Directional Airflow

Pierpaolo Puddu¹, Maurizio Paderi¹, Carlo Manca^{1*}

¹*Department of Mechanical, Chemical and Materials Engineering
University of Cagliari, Cagliari, Italy*

Abstract

This work deals with the experimental study of the flow in a Wells turbine submitted to an unsteady and bi-directional airflow. The investigations were carried out on an experimental set-up that can simulate the real operating conditions of a wave energy conversion device using a two-dimensional hot-wire anemometer probe to analyse the flow field upstream and downstream of the turbine during its non-stationary operation. In addition to local measurements, the position of the piston that simulates the wave motion, the driving torque and the turbine rotational speed were also measured. These surveys allowed determination of the turbine instantaneous performances by analysing the aerodynamic flow characteristic at mid-span in the blade-to-blade plane downstream of the rotor. The flow distribution was obtained for the phase of inflow and outflow at different values of rotational speed which was kept constant during data acquisition.

The results showed asymmetric behaviour for the two phases of intake and exhaust stroke of the piston and during acceleration and deceleration of the flow. The real entity of the hysteresis phenomenon that arose during the phases of acceleration and deceleration of the unsteady flow was evaluated considering velocity distribution in close proximity of the rotor.

© 2013 The Authors. Published by Elsevier Ltd. Open access under [CC BY-NC-ND license](https://creativecommons.org/licenses/by-nc-nd/4.0/).
Selection and peer-review under responsibility of ATI NAZIONALE

Keywords: Wells turbine; OWC system; Wave motion; Unsteady flow; Experimental investigation

* Corresponding author. Pierpaolo Puddu Tel.: +39-0706755700; fax: +39-0706755717.
E-mail address: pierpaolo.puddu@dimcm.unica.it

1. Introduction

Among the various sources of renewable energy, wave power has the highest energy potential available in the world and is easily predictable. This feature makes the resource of wave energy very attractive for contributing to satisfying the demand for electricity worldwide. To convert this energy potential into electrical energy it is important to employ particularly efficient wave motion conversion devices [1-3]. The most interesting devices designed for the extraction of wave energy are those based on the principle of the oscillating water column (OWC).

Such systems are mainly composed of two units: the system that captures and converts the energy of wave motion into pneumatic energy at lower pressure to produce a bi-directional airflow and the turbo-generator driven by this flow. This configuration presents the advantage of ensuring simplicity of construction and safety of operation.

Nomenclature

BDC	bottom dead centre
c	chord length
C_z	axial velocity component
C_t	tangential velocity component
KY	yaw coefficient
KV	velocity coefficient
p	blade pitch
P^*	static pressure coefficient
Q	flow rate
R	radius
$R_c = W c/v$	Reynolds number based on blade chord
s	circumferential position
TDC	top dead centre
T	period of wave motion
T^*	torque coefficient
$t^* = t/T$	dimensionless time
T_m	torque
U	turbine rotor velocity
V	cooling velocity
W	relative flow velocity
$Z^* = (z - z_{min}) / (z_{max} - z_{min})$	dimensionless piston position
α	absolute flow angle (with respect to tangential direction)
β	relative flow angle (with respect to tangential direction)
ΔP_s	static pressure drop
Φ	flow coefficient
ω	angular velocity
v	kinematic viscosity of air
ρ	air density
subscripts, superscripts	
1	upstream condition
2	downstream condition
θ	tangential direction
r	radial direction
t	blade tip
z	axial direction

However, the unsteady and bi-directional flow generated by the wave motion requires the use of specific turbines that can operate in such unsteady conditions. Among these, the most interesting solutions are the one proposed by A. Wells [4-6] and the impulse turbine [7-8]. Extensive investigations on these turbines have led to their aerodynamic characterization and improvement of their performance [9-12]. Although some of these studies have highlighted specific issues related to unsteady flow characteristics [13-18], most of them have been carried out with uniform flow and in stationary conditions [19-20]. In fact, unsteady turbine operation determines special problems both in flow generation and measurements of fluid dynamic and mechanical quantities characterizing turbine operation.

To take into account the non-stationary operating conditions of the Wells turbine, at the Department of Mechanical, Chemical and Materials Engineering of the University of Cagliari (DIMCM), an experimental device to simulate OWC systems was designed and built. The proposed work deals with the experimental study of the flow in a Wells turbine having NACA0015 profiles submitted to an unsteady and bi-directional airflow. In particular, a detailed aerodynamic characterization of the impeller in proximity of the rotor blading using two-dimensional hot-wire anemometer was performed. The instantaneous flow field upstream and downstream of the rotor was reconstructed and analysed in detail. The phase-locked averaging technique synchronized with the rotor passage was performed to obtain the periodic mean distribution of flow velocity at midspan in a one-blade passage for the intake and exhaust stroke of the piston. The dynamic characteristics of the turbine in terms of the dimensionless flow parameter were also determined. The hysteresis phenomenon, already pointed out by other authors [21-24], was also analysed during the phases of acceleration and deceleration of the unsteady flow.

2. Experimental set-up and instrumentation

The experimental set-up used in these investigations is shown in Fig.1. The device is composed of a piston driven by a hydraulic control unit that simulates periodic wave motion and a Wells turbine (Table 1) operating with a bi-directional airflow as in a real OWC plant. The piston, moving inside a chamber, reproduces wave motion thus generating the periodic bi-directional airflow through the turbine. To convert the mechanical energy into electrical energy, the turbine drives a three-phase induction machine controlled by an inverter with encoder feedback. The desired flow conditions can be obtained by modifying the parameters of the hydraulic control unit that control the wave characteristics of shape, amplitude and frequency of piston motion.

The set-up is instrumented with different sensors to allow measurement of torque, angular velocity, piston position and static pressure, as well as the flow characteristics upstream and downstream of the rotor using different types of probes. In this work, detailed flow characteristics are measured by introducing a two-dimensional hot-wire probe in the sections located upstream and downstream of the turbine at a distance of about 20 mm from the impeller. To perform correct measurements with a probe, the characteristic of bi-directionality of the airflow, which changes continuously during the wave period, must be taken into account.

To detect the bi-directional flow characteristics upstream and downstream of the impeller the split-fiber film DISA type 55R57 anemometer was used. The probe inserted in the sections named "piston side" and "ambient side" are conveniently oriented to allow measurement of both inlet and outlet flow from the impeller during the two phases of intake stroke of the piston "inflow" and exhaust stroke of the piston "outflow". Figure 2 shows the hot wire probe position and orientation to allow inlet and outlet flow measurements during the inflow and outflow phases. To obtain the correct information in these different flow conditions, measurements were taken in different tests.

A motorized positioning system was used to set the probe position along the blade height and to modify the orientation with respect to the flow in order to carry out measurements within the range of angular calibration of the probe. The wall static pressure measurements were taken using miniature amplified and temperature-compensated low pressure transducers, with total precision of $\pm 0.5\%$ and with a suitable operating range depending on the position of measurement (± 25 mbar and ± 100 mbar respectively for the ambient side and the piston side).

The torque measurement was performed using a cantilever load cell arranged to prevent rotation (reaction torque) of the casing of the electric machine which is supported by bearings left free to rotate. The rotational speed of the turbine was measured by an encoder and piston position by a linear potentiometer whose signal was used by the hydraulic control unit for feedback control.

Probe position and data acquisition was managed by a PC equipped with a National Instruments multifunction DAQ-board controlled with software developed in Matlab.

Since the electric driver with inverter allows control of the load and rotational speed of the impeller and the hydraulic control unit allows variation of the law of displacement of the piston, it was possible to carry out many types of tests with different operating conditions.

Several test campaigns were carried out with a periodic and bi-directional air flow through the turbine rotor generated by the reciprocating sinusoidal motion of a piston. During the tests the piston stroke was kept constant, while the period was fixed to around 9 seconds. Concerning the rotational speed of the impeller, this was maintained almost constant by the PID controller of the inverter. Different tests were carried out by changing the speed of the turbine between 50 and 80 Hz and with the Reynolds number varying between 0.8×10^5 and 1.5×10^5 . Data acquisition was performed with a sampling rate of 100 kHz, assuming a sampling time interval sufficient to complete at least one piston stroke. The signal anemometer was amplified and filtered at 10 kHz before acquisition and submitted to a phase-locked ensemble averaging technique synchronized with the rotor passage to obtain a periodic mean distribution of flow velocity in the blade passage for the inflow and outflow phases.

Measurements carried out in non-stationary operating conditions with high frequency response probes, such as the hot-wire anemometer, involve a large amount of data whose reduction is not a trivial operation.

Flow characteristics obtained in close proximity of the impeller made it possible to minimize dynamic effects due to resistive, inductive and capacitive effects of the inlet and outlet duct sections of the apparatus.

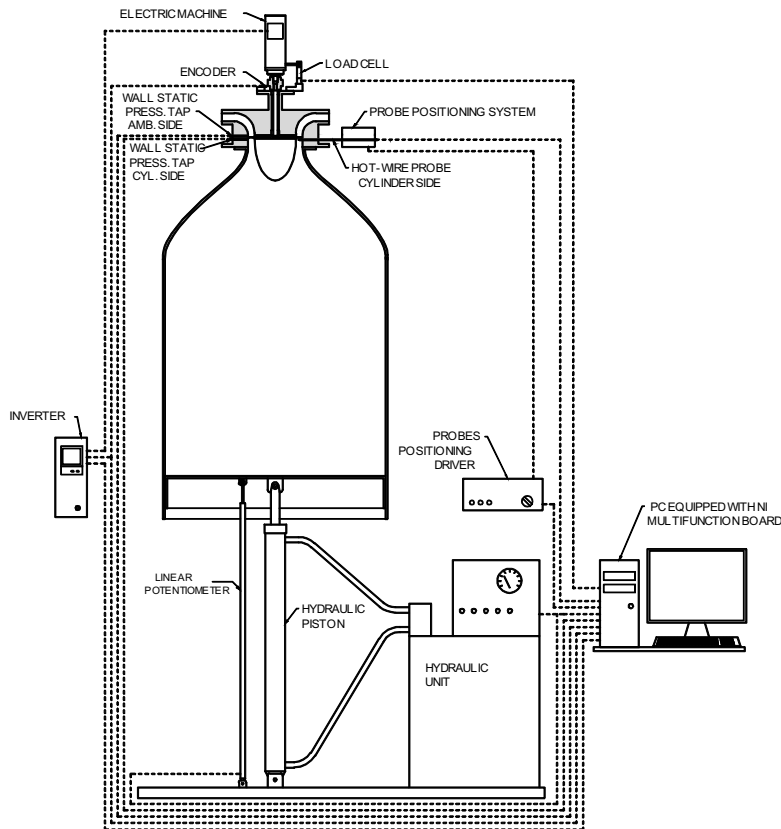


Fig. 1. Scheme of the experimental set-up and measurement chain.

Table 1 - Wells turbine geometry

Airfoil	NACA 0015
Rotor Diameter	250 mm
Hub Diameter	190 mm
Chord length	36 mm
Tip clearance	1 mm
Blade number	14
Solidity at tip radius	0.642
Sweep ratio (ratio vs. chord)	0.417 (15/36)
Rotational speed	3000-4800 rpm

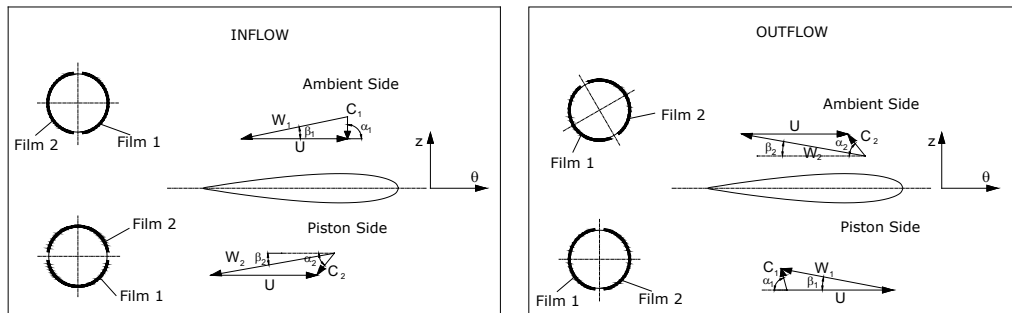


Fig. 2. Probe position and orientation upstream and downstream of the rotor blade.

3. Presentation of experimental results and analysis

Tests conducted in non-stationary conditions allowed us to obtain instantaneous flow characteristics during the inflow and outflow phases upstream and downstream of the rotor. Using the static pressure drop through the rotor and the torque at the rotor shaft, the instantaneous turbine characteristic curves during a complete period of the wave motion can be drawn.

3.1. Wells turbine characteristic curves

The characteristic curves of the Wells turbine can be represented in terms of driving torque and static pressure drop versus the instantaneous flow rate. In this set-up, characterized by the oscillating flow, the flow rate is not easy to measure; therefore it can be calculated from the piston velocity, assuming that the flow at the inlet of the turbine is axial and that the compressibility effects are negligible. Typical results for the test conducted at different rotation frequencies are reported in figure 3 for the inflow and outflow phases in terms of dimensionless coefficients, defined according to equations (1) - (3).

$$\text{Static pressure coefficient} \quad P^* = \Delta P_s / (\rho \cdot \omega^2 \cdot R_t^2) \quad (1)$$

$$\text{Torque coefficient} \quad T^* = T_m / (\rho \cdot \omega^2 \cdot R_t^5) \quad (2)$$

$$\text{Flow coefficient} \quad \Phi = C_z / (\omega \cdot R_t) = C_z / U_t \quad (3)$$

Figure 3a shows that the maximum torque coefficient is obtained in proximity of the maximum velocity of the piston and this value is greater for the outflow phase than for the inflow phase. This behaviour was observed for all different angular velocities of the turbine. At the speed of 3000 rpm, figure 3b shows that the dimensionless torque

coefficient decreases rapidly after reaching its maximum value when the flow coefficient is equal to 0.25. However, this situation does not occur at the higher rotational speed because the incidence flow angle does not reach the value that determines the stall of the profile. The same difference in torque coefficient between intake and exhaust stroke was observed in the tests conducted on the LIMPET OWC power plant [18].

Furthermore, we observed the presence of the hysteresis phenomenon between the condition of acceleration and deceleration of the flow for both phases. The hysteresis is also evident from the diagram of the static pressure coefficient besides that of torque. The hysteresis effect is slightly more pronounced for the inflow phase compared to that of outflow. To understand if hysteresis effects are due to aerodynamic behaviour of the blade profile, performance should be correlated to inlet and outlet flow characteristics. If the inlet flow is axial, the flow coefficient is univocally correlated to the angle of incidence. In the following paragraphs, hot-wire anemometer results will be used to verify if this condition is valid in the present set-up.

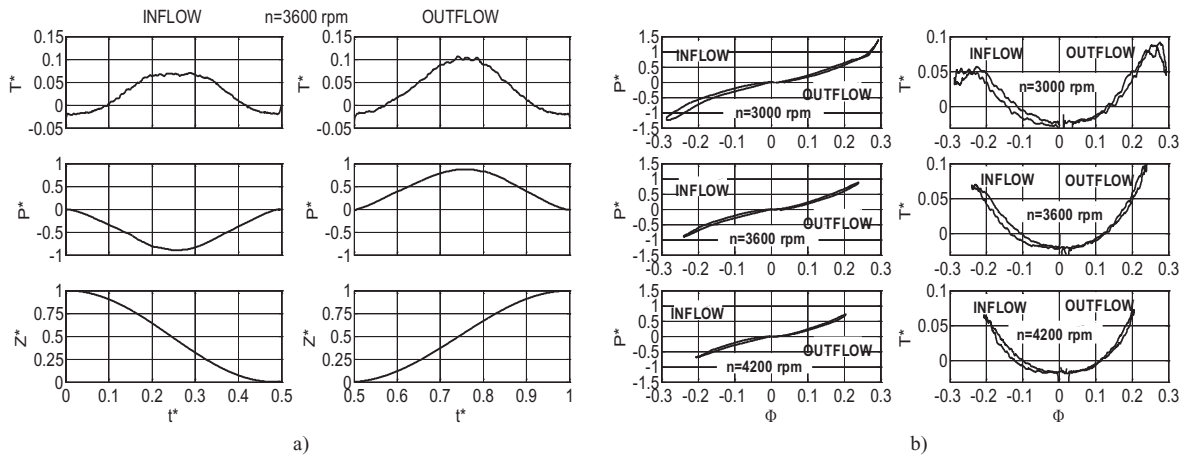


Fig. 3. Dimensionless coefficients of torque and static pressure drop for inflow and outflow phases.

3.2. Hot-wire anemometer results

The flow field, measured at the blade midspan, upstream and downstream of the impeller, is predominantly in the blade-to-blade plane because the radial velocity component can be considered negligible compared to the others as shown in [16-17]. In this way, using the 55R57 split-fiber film it is possible to obtain the instantaneous two-dimensional flow from the signal of the two films. Data reduction must be applied to the hot-wire anemometer signals: first the cooling velocities V_1 and V_2 of the two hot films are calculated from the electrical signals of the anemometer inverting King’s law. Then, the angular calibration curves, defined through the dimensionless coefficients KY and KV of equation (4), were used to evaluate the intensity of the instantaneous velocity and the flow angle in the blade-to-blade plane.

$$KY = \frac{V_2 - V_1}{V_2 + V_1} = f(\alpha) \quad KV = \frac{V_1 + V_2}{2C} = g(\alpha) \quad (4)$$

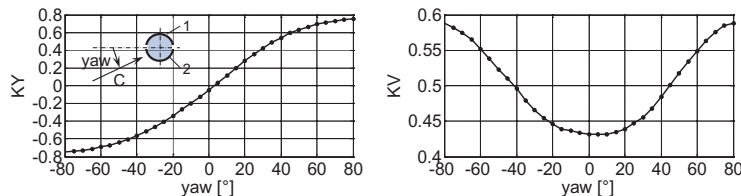


Fig. 4. Dimensionless coefficient of the angular calibration curves of 55R57 split-fiber film.

Figure 4 shows the curves of angular calibration of the DISA 55R57 split-fiber film probe used to calculate the instantaneous velocity. Taking the average of the velocity components, extended to each revolution of the impeller, we can obtain the distribution of mean velocity components versus the piston position (figure 5). These results provide a first indication of the mean flow characteristic upstream and downstream of the impeller for the two phases of the flow occurring in a complete period of oscillation of the piston.

Figure 5 shows that in the inflow phase the inlet flow can be considered axial during the entire downward phase of the piston, excluding the regions in proximity of the motion inversion. At the angular velocity of 3600 rpm, the relative flow angle β at the inlet is in all cases lower than 15° . Moreover, on increasing the rotational speed of the turbine, the incidence flow angle decreases, while the flow characteristics at the outlet of the turbine can be considered substantially unchanged and the absolute flow angle measured with respect to the tangential direction (figure 2), assumes the value of -20° . In the outflow phase, the inlet velocity to the impeller (piston side) is not axial because for the entire upward phase of the piston there is a negative tangential component of the absolute velocity and consequently the incidence flow angle is lower than that measured in the inflow phase. Such behaviour can be partially attributed to the asymmetry of the duct in proximity to the impeller but the main contribution is due to the presence of a swirling flow of air inside the cylinder created by the previous inflow phase. These results confirm that the rotor experiences a different flow deflection and consequently a different circulation and lift coefficient is generated during the inflow and outflow phases.

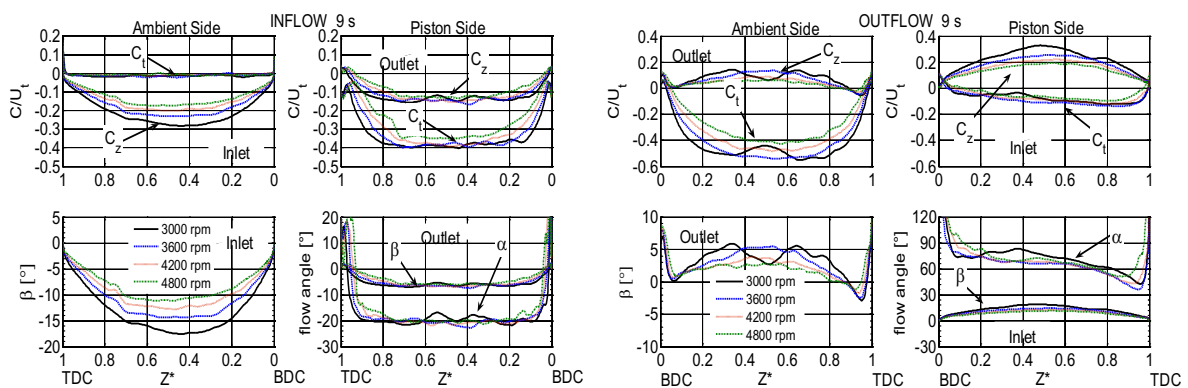


Fig. 5. Mean flow characteristics at the blade mid-span for the inflow and outflow phases (3600 rpm).

Although the motion of the piston is perfectly symmetrical, the two active phases do not guarantee identical performance and the flow field characteristics are different. On increasing the rotational speed, the flow characteristics do not change substantially: the incidence flow angle shows a reduction while at the impeller outlet a small reduction of the tangential velocity component is observed.

The presence of a non-axial flow at the inlet of the turbine during the outflow phase, as already highlighted in [16], justifies the different performance of the turbine between the inflow and outflow phases. To directly correlate the dimensionless coefficients of static pressure and torque with the angle of incidence of the mean flow, the results of the hot-wire anemometer tests at the blade midspan were used. Figure 6 reports the dimensionless coefficients as a function of the relative flow angle at the inlet of the turbine for the two phases and for different angular velocities of the impeller. This representation is very similar to that shown in figure 3b but in this case the incidence flow angle for the outflow phase is not directly correlated to the flow coefficient.

The different performance of the turbine between the two phases of flow is quite evident in these graphs as well. Furthermore, figure 6 highlights different performances during the acceleration and deceleration of the flow only for the outflow phase.

The pressure coefficient and the torque coefficient show higher values for the deceleration phase of the flow (reduction of β) with respect to the phase of acceleration (increase of β) only during the outflow phase, while in the inflow phase the hysteresis is negligible. Such results are in agreement with those presented in [16] even though the analysis was limited only to the inflow phase.

It is important to note that the true amount of hysteresis is less than that observed previously when the same coefficients were represented in function of the flow coefficient calculated from the law of displacement of the piston. In fact, in this case the dimensionless coefficients of the turbine are directly related to the flow angle at the inlet of the turbine, thereby avoiding the delay effects introduced by the presence of ducts and chamber.

From figure 6 it is clear that when the angle of the relative flow exceeds 15° , the dynamic stall of the profile occurs at the rotational speed of 3000 rpm. At a higher velocity the angle of incidence is smaller and the stall condition is never achieved. However, to obtain high positive torque, the inlet flow angle must be close to the stall condition value.

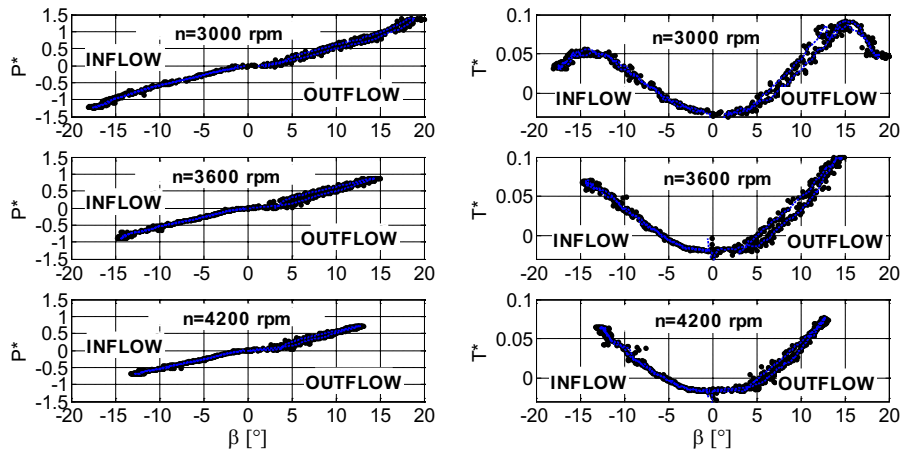


Fig. 6. Dimensionless torque coefficient as a function of the angle of incidence

In ref. [22] the hysteresis effect is attributed to the different interaction between the wake and the suction side of the profile. When the relative flow angle β at the exit of the rotor is small, the interaction increases and the hysteresis effect is more pronounced. To verify the effects of interaction between wakes and profiles, detailed measurements downstream of the turbine were carried out using the hot-wire anemometer.

The instantaneous velocities obtained from the signals of the hot-wire anemometer can be processed to obtain periodic mean value of the velocity components upstream and downstream of the impeller in one blade pitch. The instantaneous velocity was triggered off-line using the digital signal of the optical encoder employed to detect impeller velocity. In this way, the phase-locked ensemble averaging technique was applied to obtain a periodic mean distribution of the flow velocity in the blade passage for the inflow and outflow phases. However, the averaging process must be applied carefully because the measurements were carried out in non-stationary flow conditions. To obtain reliable results, the ensemble average was extended to a convenient time interval or to a reasonable number of revolutions of the impeller to confirm that the intake flow can be considered almost constant during the averaging process. The best choice is a compromise between a small number of revolutions, which ensure a substantially constant operating condition but worse averaging results, and a large number of revolutions, which produce a good averaging result but extended to operating conditions that can no longer be regarded as constant. Another important issue that must be considered during the averaging process is the fluctuation of the angular velocity of the turbine. In this situation the phase-locked ensemble average was correctly applied considering the same spatial position in the blade pitches.

The analysis was conducted for three different operating conditions in the half-period of motion of the piston: the first P_1 corresponds to the position of maximum speed, P_2 in the acceleration phase and P_3 in the deceleration phase of the flow, characterized by the same incidence flow angle. The three positions are represented in figure 7 along the displacement of the piston.

The results of figure 7 were obtained performing the ensemble average of data acquired in a time interval of less than 0.1 s, corresponding to only 5 revolutions of the rotor or 70 complete blade pitches. The distribution of the velocity components and relative flow angle shows periodic behaviour determined by the blade passage. In the case

of inflow, the inlet flow is axial in all three points examined: the axial velocity and the incidence flow angle assumes the maximum value at point P_1 while the flow at points P_2 and P_3 , respectively in the accelerating and decelerating phases, are chosen with the same angle of incidence. In this way, the relative flow angle reaches the value of -15° at point P_1 (value close to incipient stall of the profile), while the incidence flow angle is around -8° at points P_2 and P_3 . The relative flow angle at the outlet of the turbine shows a small oscillation between -5° and -7° at point P_1 while at points P_2 and P_3 there is no evident difference, thus confirming that the effect of hysteresis between the phase of acceleration and that of deceleration is negligible.

In the case of outflow, at point P_1 the inlet axial velocity component again assumes the maximum value, but also evident is the presence of a negative tangential velocity component which is higher during flow deceleration (point P_3). In the phase of acceleration (point P_2), the angle of incidence grows and the outlet flow angle β_2 is higher than that measured during the deceleration phase (point P_3), where the angle of incidence decreases. Therefore, a lower deflection angle at point P_2 with respect to point P_3 is reached and, because the lift coefficient is closely connected with the deflection angle, the circulation during the acceleration phase is less than that of the deceleration phase. This behaviour can be explained by assuming that during the acceleration phase the increase in circulation, due to the increase of incidence, occurs with a delay, thus penalizing performance. Similarly, during flow deceleration, the reduction in circulation is delayed with respect to the reduction of the incidence, thus maintaining a high performance and thereby determining the effect of hysteresis. This behavior is in agreement with the presence of the hysteresis observed in the distribution of the torque coefficient reported in function of the incidence flow angle for the outflow phase in figure 6.

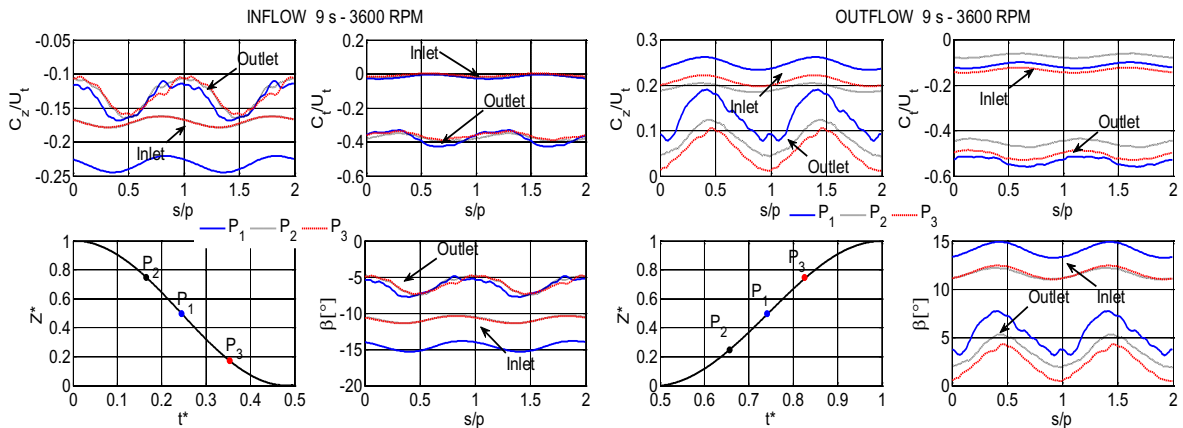


Fig. 7. Periodic flow upstream and downstream of the rotor along a blade pitch for inflow and outflow phases.

Conclusions

Results obtained from an experimental flow investigation in a Wells turbine submitted to a bi-directional flow are presented and analysed. The real non-stationary operating conditions of the OWC devices are taken into account using an experimental set-up able to generate a bi-directional airflow through the turbine. A two-dimensional hot-wire anemometer probe was inserted upstream and downstream of the rotor to obtain instantaneous information about the aerodynamic performance of the turbine. The performance of the Wells turbine is presented using the dimensionless coefficients of static pressure drop through the rotor and driving torque versus the incident flow angle of the relative velocity.

Many tests were carried out at fixed time periods of 9 s and at different rotational velocities of the turbine for both inflow and outflow phases. Results obtained can be summarized as follows:

- the turbine performs better during the outflow phase compared to the inflow phase. This difference is due to the asymmetry of the inlet flow between the two phases. During the outflow phase a high tangential velocity component at the inlet of the impeller is present. Such behaviour can be partially attributed to the

- asymmetry of the duct in proximity to the impeller and mainly to the presence of a swirling flow of air inside the cylinder caused by the previous phase of inflow;
- the real characteristics of the hysteresis are obtained by plotting the dimensionless coefficients as a function of the angle of incidence of the flow obtained from the measurements of the probe in proximity to the rotor inlet during the inflow and outflow phases. The hysteresis can be noticed only during the outflow phases and is negligible in the inflow phase;
 - the ensemble average of the hot-wire measurements made it possible to provide detailed information on the aerodynamic behavior of the Wells turbine. The periodic trend of the velocity components and flow angle in a blade pitch have confirmed and justified the presence of the hysteresis effect, especially during the phase of outflow, where higher performance was obtained during flow deceleration compared to that of acceleration.

References

- [1] Thorpe, T., Wave Energy for the 21st century. Status and prospects, *Renewable Energy World*, 2000; 115-121-July-August
- [2] Taylor R. H. *Alternative Energy Sources for the centralised generation of electricity*, Adam Hilger Ltd, Bristol, 1983
- [3] Falcão A. F. de O., Wave energy utilization: A review of the technologies, *Renewable and Sustainable Energy Reviews*, 2010; 14:899-918
- [4] Wells A. Fluid driven rotary transducer - Br. Pat. 1595700, 1976
- [5] Raghunathan S., The Wells turbine for wave energy conversion, *Progress in Aerospace Sciences*, 1995; 31:335-386
- [6] Gato L. M. C Falcão A. F. de O., Aerodynamics of the Wells turbine, *J. Mech. Sci.* 1988; 30:383-395
- [7] Setoguchi T., Santhakumar S., Maeda H., Takao M., Kaneko K., A review of impulse turbines for wave energy conversion, *Renewable Energy*, 2001; 23:261-292
- [8] Setoguchi T., Takao M., Current status of self rectifying air turbines for wave energy conversion, *En. Conv.and Man.* 2006; 47:2382-2396
- [9] Raghunathan S., Tan C. P., Ombaka O. O., Performance of the Wells self-rectifying air turbine, *Aeronautical Journal (ISSN 0001-9240)*, 1985; 89:369-379
- [10] Curran R. Gato L. M. C., The energy conversion performance of several types of Wells turbine designs, *Proceedings of the Institution of Mechanical Engineers, Part A, Journal of Power and Energy*, 1997; 211:133-145
- [11] Kim T. H., Setoguchi T., Takao M., Kaneko K., Santhakumar S., Study of turbine with self-pitch-controlled blades for wave energy conversion, *Int. J. of Thermal Sci.* 2002; 41:101-107
- [12] Setoguchi T., Santhakumar S., Takao M., Kim T.H., Kaneko K., A modified Wells turbine for wave energy conversion, *Renewable Energy* 2003; 28:79-91
- [13] Camporeale S. M., Filianoti P., Behaviour of a small Wells turbine under randomly varying oscillating flow, *Proceedings of the 8th European Wave and Tidal Energy Conference*, 2009; Uppsala
- [14] Filianoti P., Camporeale S. M.. In field measurements on a small scale OWC device, *Proceedings of the 8th European Wave and Tidal Energy Conference*, 2009; Uppsala
- [15] Thakker A., Abdulhadi R., The performance of Wells turbine under bi-directional airflow, *Renewable Energy* 2008; 33:2467-2474
- [16] Paderi M., Puddu P., Experimental investigation in a Wells turbine under bi-directional flow, *Renewable Energy* 2013; 57:570-576
- [17] Nurzia F., Paderi M., Puddu P., Caratterizzazione sperimentale di un simulatore di moto ondoso con turbina Wells, Domus de Maria (CA) *Congresso Nazionale ATI*; 2010
- [18] Folley M, Curran R, Whittaker T, Comparison of LIMPET contra-rotating wells turbine with theoretical and model test predictions, *Ocean Engineering* 2006; 33:1056-1069
- [19] Raghunathan S., Tan C. P., Wells N. A. J., Wind tunnel tests on airfoils in tandem cascade, *AIAA Journal*, 1981; 19:1490-1492
- [20] Curran R, Gato L., The energy conversion performance of several types of Wells turbine design, *Proc. Instn. Mech. Engrs.* 1997; part. A 112:133-145
- [21] Kinoue Y., Kim T.H., Setoguchi T., Mohammad M., Kaneko K., Inoue M.. Hysteretic characteristics of monoplane and biplane Wells turbine for wave power conversion, *Energy Conversion and Management* 2004, 45:1617-1629
- [22] Setoguchi T., Takao M., Kaneko K., Hysteresis on Wells turbine characteristics in reciprocating flow, *Int. J. of Rotating Machinery*, 1998; 4:17-24
- [23] Setoguchi T., Kinoue Y., Kim T.H., Kaneko K., Inoue M., Hysteretic characteristics of Wells turbine for wave power conversion, *Renewable Energy* 2003; 28:2113-2127
- [24] Kim T.H., Kinoue Y., Setoguchi T., Kaneko.K., Effects of Hub To Tip Ratio and Tip Clearance on Hysteretic Characteristics of Wells Turbine for Wave Power Conversion, *Journal of Thermal Science*, 2002; 11:207-2013